International Journal of Remote Sensing
Vol. 26, No. 18, 20 September 2005, 3901–3910

Taylor & Francis
Taylor & Francis Group

Derivation of terrain roughness indicators via granulometries

L. T. TAY*†, B. S. DAYA SAGAR‡ and H. T. CHUAH†
†Faculty of Engineering, Multimedia University, Cyberjaya Campus, Jalan Multimedia, 63100 Cyberjaya, Selangor, Malaysia
‡Faculty of Engineering and Technology, Melaka Campus, Multimedia University, Jalan Ayer Keroh Lama, 75450, Melaka, Malaysia

(*Received 4 February 2005; in final form 17 February 2005*)

Digital elevation models (DEMs) provide rich clues about various geophysical and geomorphologic processes. These clues include conspicuous protrusions and intrusions of foreground and background portions that testify the presence of channels and ridges in DEMs. We show an application of greyscale granulometries to characterize DEMs through shape–size complexity measures relative to symmetric rhombus, octagon and square templates. We first compute pattern spectra that measure the size distributions of protrusions and intrusions in a DEM. We then employ pattern spectra to compute probability size distribution functions of protrusions and intrusions relative to three templates. We finally compute shape–size complexity measures of DEM by employing these probability functions. To illustrate the implementation of granulometric approach to compute these measures of both background and foreground, we consider an interferometrically generated DEM of a part of Cameron Highlands of Malaysia. Hierarchical watersheds that could be decomposed from DEMs can be better classified via these measures.

1. Introduction

Terrain roughness indicates several surficial processes and characteristics. Characterization of such roughness for geological and geomorphologic research hitherto can be done by several methods (e.g. Horton 1945, Stone and Dugundji 1965, Daniels *et al.* 1970, Franklin 1987, Ackeret 1990). Several earlier studies characterized terrain or watersheds by analysing the spatial organization of the unique channel and ridge connectivity networks that could be retrieved from digital elevation models (DEMs), which are defined as functions representing spatially distributed elevations in grey levels. Higher and lower category elevations represent brighter and darker grey levels, respectively. Morphometry, fractal and allometric scaling analyses of such networks provide various characteristics in a quantitative manner (Horton 1945, Langbein 1947, Rodriguez-Iturbe and Rinaldo 1997, Turcotte 1997, Sagar *et al.* 1998a, Maritan *et al.* 2002, Sagar and Tien 2004, Sagar and Chockalingam 2004). Precise derivation of DEMs from remotely sensed data has shown significant success in terrain characterization studies. The importance of DEMs in understanding geological and geomorphologic processes has since been realized (e.g. Montgomery and Foufoula-Georgiou 1993, Rodriguez-Iturbe and Rinaldo 1997, Whipple and Tucker 1999, Whipple *et al.* 1999, Snyder *et al.*

*Corresponding author. Email: lttay@mmu.edu.my

International Journal of Remote Sensing
ISSN 0143-1161 print/ISSN 1366-5901 online
http://www.tandf.co.uk/journals
DOI: 10.1080/01431160500165880

2000, Dall *et al*. 2001, Rodriguez *et al.* 2002, Baratoux *et al*. 2002, Dadson *et al*. 2003). With the advent of powerful computers and high resolution remotely sensed data capable of generating DEMs, it is now possible to characterize surficial features by means of advanced mathematical concepts, one of which includes mathematical morphology (Matheron 1975, Serra 1982). Applications of mathematical morphologic concepts shown in the context of geomorphology include extraction of significant geomorphologic features from digital elevation models (Sagar 2001a, Sagar *et al*. 2000, 2003), estimation of basic measures of water bodies (Sagar *et al*. 1995a, b), modelling and simulation of geomorphic processes (Sagar *et al*. 1998b, Sagar 2001b, 2005), generation of fractal landscapes (Sagar and Murthy 2000), and fractal relationships among various parameters of geomorphologic interest (Sagar 1996, 1999, 2000, Sagar *et al*. 1998b, 1999, 2001, Sagar and Chockalingam 2004, Sagar and Tien 2004). It is proposed in this paper to derive shape–size complexity measures, such as average size and roughness from DEM.

A DEM provides a three-dimensional representation of earth terrain, vital in geographical and remote sensing information. Global high quality and good resolution DEMs can be generated using elevation data derived from contour maps, digitized elevation maps, stereo models based on remote sensing images, and new technologies such as radar interferometry (Zebker and Goldstein 1986), and laser altimetry (Ritchie 1995). Recently high-resolution DEM data of the Earth on a near-global scale have been produced by Shuttle Radar Topography Mission (SRTM) (Farr and Kobrick 2000). DEMs in spatio-temporal mode are derived from remote sensing data of various acquisition sources. Processing of such DEMs has offered many approaches in terrain characterization. This enables new understanding in earth surface processes.

The motivation for this study relies on addressing the following questions:

(a) What do bright and dark regions represent in a DEM?
(b) How do bright and dark regions of a DEM transform with multiscaling?
(c) How do granulometries characterize terrain?
(d) How do shape–size complexity measures of bright and dark regions characterize a DEM?

This work is based on computations of area lost in DEMs across successive resolutions. This lost information, which includes protrusions and intrusions of various sizes, is computed as the area of the portion obtained from subtracting the DEMs of successive resolutions. For this purpose, we generate multiscale DEMs via multiscale openings and closings. Furthermore, the loss of information obtained would be used to compute probability functions, based on which average size and average roughness are estimated.

2. Study region, definitions and transformations

The study region is situated between the geographical co-ordinates of 4°31′–4°34′ N and 101°16′–101°19′ E in a mountainous forest located in the east part of Perak in Peninsular Malaysia. The geology of this region is granite rocks occupied by small portions of metamorphic rocks, and alluvium covers most of the area. The DEM of this region (figure 1(*a*)), encompassing an area of 600×600 pixels (one pixel is $10\,\text{m} \times 10\,\text{m}$), is represented by a function, f. Let $f(x,y)$ be a function of Z^2, and B be a fixed element of size one (figure 1(*b*)). The erosion (dilation) of f by B replaces the

value of f at a pixel (x, y) by the minima (maxima) of the values of f over a structuring template B ($\hat{B}$ is B rotated about 180°). In the present case, we consider $B = \hat{B}$. We represent these grey level morphological transformations as:

$$(f \ominus B)(x, y) = \min_{(i,j)\in B} \{f(x+i, y+j)\} \tag{1}$$

$$(f \oplus B)(x, y) = \max_{(i,j)\in B} \{f(x-i, y-j)\}, \tag{2}$$

where B is a discrete binary template (e.g. figure 1(*b*)), and $\ominus$ and $\oplus$ denote symbols for erosion and dilation. In other word, $(f \ominus B)$ and $(f \oplus B)$ can be obtained by computing minima and maxima over a moving template B, respectively. The grey level opening and closing of f by B are the functions $(f \circ B) = [(f \ominus B) \oplus B]$ and $(f \bullet B) = [(f \oplus B) \ominus B]$, where $\circ$ and $\bullet$ denote symbols for opening and closing, respectively.

Subsequently, multiscale opening and closing are performed by increasing the size (scale) of the structuring template B_n, where $n = 0, 1, 2, \ldots, N$. These multiscale openings and closings of f by B are represented as (i) $\{[(f \ominus B) \ominus B \ominus \ldots \ominus B] \oplus B \oplus B \oplus \ldots \oplus B\} = [(f \ominus B_n) \oplus B_n] = (f \circ B_n)$ and (ii) $\{[(f \oplus B) \oplus B \oplus \ldots \oplus B] \ominus B \ominus B \ominus \ldots \ominus B\} = [(f \oplus B_n) \ominus B_n] = (f \bullet B_n)$ at scale $n = 0, 1, 2, \ldots, N$, respectively. Performing opening and closing iteratively by increasing size of B transforms the DEM into respective lower resolutions. Multiscale opening and closing of DEM by B_n affect spatially distributed elevation regions in the form of smoothing of contours to various degrees. The shape and size of B control the shape of smoothing and the scale, respectively.

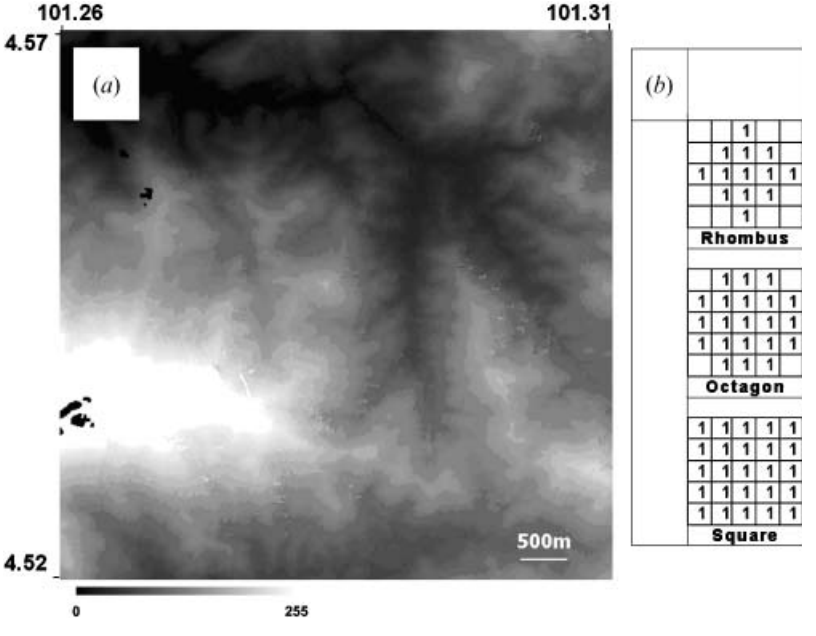

Figure 1. (*a*) DEM of a part of Cameron Highlands, Malaysia, and (*b*) disk-like structuring templates in different connectivity grids.

3. Granulometry of DEM via opening and closing

Local foreground and background in the DEM signify higher and lower local elevations, respectively. Granulometries by opening and closing of DEM produce DEMs at multiple scales, where various sizes of protrusions and intrusions from foreground and background structures would be filtered out correspondingly. The basic difference between performing opening and closing to generate DEMs at multiple resolutions lies in the objective of computing roughness of foreground (essentially due to local lower elevations) and background (essentially due to local higher elevations). These multiscale DEMs provide basic information to compute shape–size complexity measures.

We perform multiscale openings and closings on Cameron Highlands DEM by means of symmetric rhombus, octagon and square templates, which are disks in 4- and 8-connectivity square grids (figure 1(*b*)). An octagon of size 5×5 is the Minkowski sum of a square and rhombus of size 3×3. Illustrations of specific resultant multiscale DEMs at multiple scales can be seen in figure 2. We observe large flat plateaus (figure 2(*a*)) and flat sinks (figure 2(*b*)) shaped like B_n at large scales n of the opening ($f \bigcirc B_n$) and the closing ($f \bullet B_n$), respectively. The area of the multiscale opening DEMs, $A(f) = \sum_{(x,y)} f(x, y)$, decreases with increasing opening cycle and $A(f \bigcirc B_0) \geqslant A(f \bigcirc B_1) \geqslant A(f \bigcirc B_2) \geqslant \ldots \geqslant A(f \bigcirc B_n) = A(f \bigcirc B_{n+1})$. Similarly, the area of the multiscale closing DEMs increases with increasing closing cycle, which is mathematically shown as $A(f \bullet B_0) \leqslant A(f \bullet B_1) \leqslant A(f \bullet B_2) \leqslant \ldots \leqslant A(f \bullet B_n) = A(f \bullet B_{n+1})$.

We compute areas of protrusions and intrusions from Cameron Highlands DEM that are filtered out at respective scales as a main parameter to estimate the shape–size complexity measures by means of symmetric templates. Thus, we employ pattern spectra (Maragos 1989) that map each size n to some measure of the higher order of f relative to B as:

$$PS_f(+n, B) = A[(f \bigcirc B_n) - (f \bigcirc B_{n+1})],\ 0 \leq n \leq N \tag{3}$$

$$PS_f(-n, B) = A[(f \bullet B_n) - (f \bullet B_{n-1})],\ 1 \leq n \leq K, \tag{4}$$

where $PS_f(+n, B)$ and $PS_f(-n, B)$ are the pattern spectra of foreground and background portions of f relative to B, and $a(x) - b(x)$ is the point-wise algebraic difference between the two functions $a(x)$ and $b(x)$. The information that we compute by subtracting each opened version from the preceding level of opened version are the protrusions of size smaller than the B_n that could be filtered via corresponding level of opening (equation (3)). By incorporating multiscale closings, we estimate the pattern spectrum of negative size portions by taking into account the complexity of the local background of f. We obtain intrusions by subtracting the closed version from its succeeding level (equation (4)). The unions of these protrusions and intrusions testify the presence of channels and ridges. In other words, we compute the difference between the area after nth level opened DEM and the area after $(n+1)$th level opened DEM (where n ranges from 0 to N). This difference is divided by the area of the original DEM, $A(f)$, to get the probability function at nth level, $ps(n, f)$. This descriptive procedure is given with a mathematical

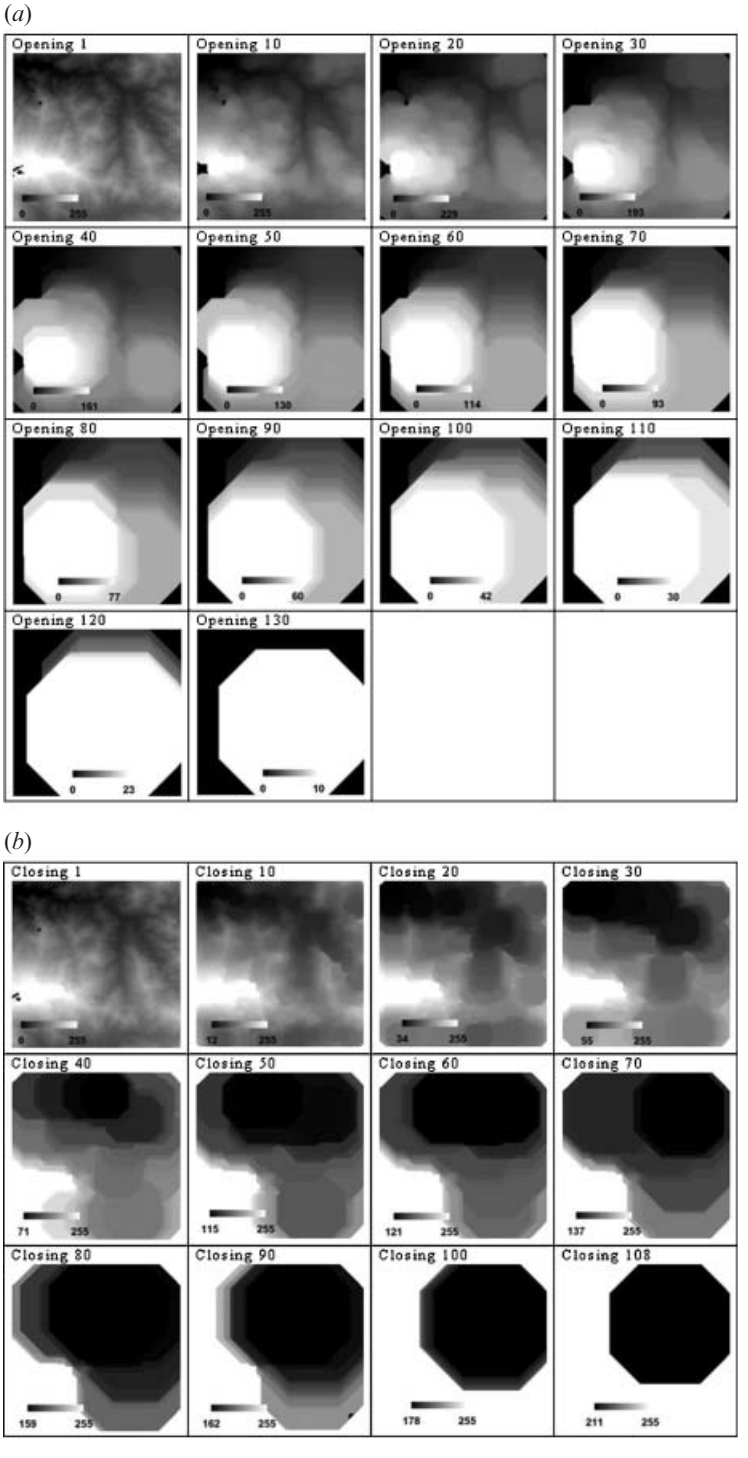

Figure 2. Multiscale DEMs generated via granulometries by opening and closing at different levels. The interval between the contiguous levels is considered to be 10 (the structure element used is the octagon).

abstraction as:

$$ps(n, f) = \frac{A(f \bigcirc B_n) - A(f \bigcirc B_{n+1})}{A(f \bigcirc B_0)},\ n = 0, 1, 2, \ldots, N, \tag{5}$$

where $0 \leqslant ps(n, f) \leqslant 1$. In other words, the probability function is the ratio between the area of the region that is obtained from algebraic difference between contiguous levels of opened DEM and the area of DEM. These filtered features of f with size B_n are a sort of crenulation protruding above f. This further implies that the larger the $ps(n, f)$, the more features with size B_k protrude above f. A $ps(n, f)$ value of 0 indicates that there are no features of size B_k. However, a value of 1 for $ps(n, f)$ indicates that there exists one only feature protruding above f, and its size is B_N. We also compute the difference between the area after nth level closed DEM and the area after $(n-1)$th level closed DEM (where n ranges from 1 to N). This difference is divided by $A(f)$ to get the probability function at nth level, $ps(-n, f)$. This is mathematically expressed as:

$$ps(-n, f) = \frac{A(f \bullet B_n) - A(f \bullet B_{n-1})}{A(f \bullet B_k)}, \tag{6}$$

where $0 \leqslant ps(-n,\ f) \leqslant 1$. To compute the shape–size complexity measures of background region in Cameron Highlands DEM, the probability function (equation (6)) is computed as the ratio between the area of the region obtained from algebraic difference between contiguous levels of closed DEM and the area of DEM.

4. Shape–size complexity measures

Shape–size complexity measures include average size and roughness of a DEM. The basic information needed to compute these two measures includes the areas estimated from the granulometric analysis and the normalized probability functions (figure 3). These scalar independent measures that rely on topological and geometrical criteria can be considered as indicators, in order to understand the complexity of surface due to size distributions of protrusions/intrusions. Therefore, we compute $ps(n, f)$ and $ps(-n, f)$ for DEM in a normalized way. We estimate average size, $AS(f/B)$, and average roughness, $H(f/B)$, of foreground by incorporating $ps(n, f)$ relative to B as:

$$AS(f/B) = \sum_{n=0}^{N} nps(n, f) \tag{7}$$

$$H(f/B) = -\sum_{k=0}^{n} ps(n, f) \log ps(n, f). \tag{8}$$

To compute similar measures of the background of f, we consider $ps(-n, f)$ of background portions of f, estimated according to equation (6). Average roughness quantifies the shape–size complexity of f by means of its surface roughness, due to the protrusion and intrusion distribution averaged over all depths that B reaches.

For instance, a triangular shape, while investigating through granulometries by opening with triangular template, which is homothetic to triangle, yields a higher

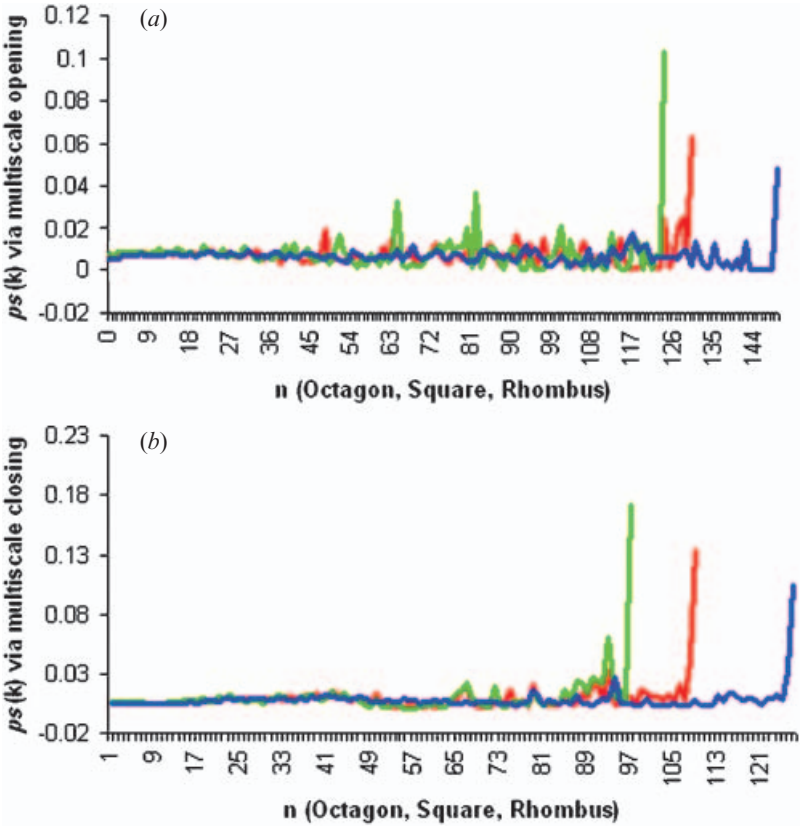

Figure 3. Graphical plot of size of structuring element and normalized probability functions estimated from granulometries via (*a*) opening and (*b*) closing. Blue, red and green are, respectively for rhombus, octagon and square.

value for average size, and a lower value for roughness, than those of other non-homothetic templates. To illustrate this point on a greyscale DEM, three templates are used in this investigation.

We derive the indexes of $AS(f/B)$ and $H(f/B)$ (table 1) for the DEM with granulometries by opening and closing using three disk-like templates. We compute $AS(f/B)$ from the probability functions estimated with granulometries by opening and closing using rhombus, octagon and square, respectively, and obtain 73.40, 68.30 and 64.90 (opening), and 72.43, 67.26 and 63.33 (closing). Based on the granulometric analysis of DEM through openings relative to rhombus, octagon and square, $H(f/B)$ is estimated for Cameron Highlands DEM as 6.99, 6.72 and 6.36, respectively. Similar analysis via closing by means of the three templates yields $H(f/B)$ values of 6.59, 6.15

Table 1. Shape–size complexity measures of a DEM.

	$AS(f/B)$			$H(f/B)$		
Multiscale	Rhombus	Octagon	Square	Rhombus	Octagon	Square
Opening	73.40	68.30	64.90	6.99	6.72	6.36
Closing	72.43	67.26	63.33	6.59	6.15	5.78

and 5.78, respectively. The higher the $H(f/B)$, the higher is the maximal pattern B_n at equal area portion in all sizes n that f contains. An $H(f/B)$ value close to zero indicates that f is the union of maximal patterns of one size.

As the $AS(f/B)$ value estimated for f relative to B increases, so does the $H(f/B)$ value relative to the same B. This is obvious from table 1. As the highest $H(f/B)$ value estimated via opening (closing), i.e. 7 (6.6), is due to rhombus, the estimated $AS(f/B)$ value via opening (closing) relative to the rhombus is the largest among the three values, i.e. 73.40 (72.43). We also observe that the smaller the number of elements in a symmetric template, the higher are the average size and roughness values, and vice versa. These measures relative to symmetric templates provide overall characteristics of DEMs. Based on these measures, which are sensitive to changes in the characteristic information of B, one can make a clear demarcation between the terrains. From the characteristic information point of view, in general, there is a clear distinction between symmetric and asymmetric templates. Such a distinction leads to different results. However, we hypothesize that such a distinction would be useful to understand direction- and location-specific shape–size complexity measures within a watershed. Changes in characteristic information such as those in terms of shape, size, origin and orientation can be employed to unravel characteristic dependent shape–size content from the DEM. Application of other choices of templates that can be used instead of disks to unravel the desired topological properties of watersheds will be addressed in our future work.

5. Conclusions and scope

In this study, we perform granulometric analysis via opening and closing to filter the protrusions and intrusions of both foreground and background that are conspicuous in Cameron Highlands DEM. Two indexes to quantify shape–size content in foreground and background portions of the DEM are computed. Further, we hypothesize that the computed indexes correlate well with the dimensions of channel and ridge networks that summarize connectivity, orientation, and association of concave and convex regions of several orders in DEMs. Sub watershed-wise granulometric analysis and estimation of these measures, which are sensitive to surficial changes, would facilitate new insights into classifying watersheds. With the advent of robust tools to derive relatively error-free DEMs from multi-temporal (scale) remotely sensed data, linking surficial processes involved in shaping the terrain with respect to these complexity measures is a potentially valuable study that needs further investigation.

Acknowledgments

We gratefully acknowledge the help provided by the Malaysian Centre for Remote Sensing (MACRES) in providing Cameron Highlands DEM data and Professor Arthur P. Cracknell for providing useful comments and suggestions.

References

Ackeret, J.R., 1990, Digital terrain elevation data resolution and requirements study. Interim Report ETL-SR-6, US Army Corps of Engineers.

Baratoux, D., Mangold, N., Delacourt, C. and Allemand, P., 2002, Evidence of liquid water in recent debris avalanche on Mars. *Geophysical Research Letters*, **29**, p. 1156.

DADSON, S.J., HOVIUS, N., CHEN, H., DADE, B., HSIEH, M.L., WILLETT, S.D., HU, J.C., HORNG, M.J., CHEN, M.C., STARK, C.P., LAGUE, D. and LIN, J.C., 2003, Links between erosion, runoff variability and seismicity in the Taiwan region. *Nature*, **426**, pp. 648–651.

DALL, J., MADSEN, S.N., KELLER, K. and FORSBERG, R., 2001, Topography and penetration of the Greenland ice sheet measured with airborne SAR interferometry. *Geophysical Research Letters*, **28**, pp. 1703–1706.

DANIELS, R.B., NELSON, L.A. and GAMBLE, E.E., 1970, A method of characterizing nearly level surfaces. *Zeitscheift fur Geomorphologies*, **14**, pp. 175–185.

FARR, T. and KOBRICK, M., 2000, Shuttle radar topography mission produces a wealth of data. *Eos Transactions AGU*, **81**, pp. 583–585.

FRANKLIN, S., 1987, Geomorphometric processing of digital elevation models. *Computers and Geosciences*, **13**, pp. 603–609.

HORTON, R.E., 1945, Erosional development of streams and their drainage basins: hydrophysical approach to quantitative morphology. *Bulletin of the Geophysical Society of America*, **56**, pp. 275–370.

LANGBEIN, W.B., 1947, Topographic characteristics of drainage basins. US Geologocal Survey Professional Paper 968–C.

MARAGOS, P.A., 1989, Pattern spectrum and shape representation. *IEEE Transactions on Pattern Analysis and Machine Intelligence*, **11**, pp. 701–716.

MARITAN, A., RIGON, R., BANAVAR, J.R. and RINALDO, A., 2002, Network allometry. *Geophysical Research Letters*, **29**, p. 1505.

MATHERON, G., 1975, *Random Sets and Integral Geometry* (New Jersey: John Wiley Hoboekn).

MONTGOMERY, D.R. and FOUFOULA-GEORGIOU, E., 1993, Channel network source representation using digital elevation models. *Water Resources Research*, **29**, pp. 3925–3934.

RITCHIE, J.C., 1995, Airborne laser altimeter measurements of landscape topography. *Remote Sensing of Environment*, **53**, pp. 85–99.

RODRIGUEZ, Z.F., MAIRE, E., COURJAULT-RADE, P. and DARROZES, J., 2002, The black top hat function applied to a DEM: a tool to estimate recent incision in a mountainous watershed (Estibere Watershed, Central Pyrenees). *Geophysical Research Letters*, **29**, Art. No. 1085.

RODRIGUEZ-ITURBE, I. and RINALDO, A., 1997, *Fractal River Basins: Chance and Self-organization* (Cambridge: Cambridge University Press).

SAGAR, B.S.D., 1996, Fractal relations of a morphological skeleton. *Chaos, Solitons and Fractals*, **7**, pp. 1871–1879.

SAGAR, B.S.D., 1999, Estimation of number-area-frequency dimensions of surface water bodies. *International Journal of Remote Sensing*, **20**, pp. 2491–2496.

SAGAR, B.S.D., 2000, Fractal relation of medial axis length to the water body area. *Discrete Dynamics in Nature and Society*, **4**, p. 97.

SAGAR, B.S.D., 2001a, Generation of self organized critical connectivity network map (SOCCNM) of randomly situated surface water bodies. *Discrete Dynamics in Nature and Society*, **6**, pp. 225–228.

SAGAR, B.S.D., 2001b, Hypothetical laws while dealing with effect by cause in discrete space. *Discrete Dynamics in Nature and Society*, **6**, pp. 67–68.

SAGAR, B.S.D., 2005, Discrete simulations of spatio-temporal dynamics of small water bodies under varied streamflow discharges. *Nonlinear Processes in Geophysics*, **12**, pp. 31–40.

SAGAR, B.S.D. and CHOCKALINGAM, L., 2004, Fractal dimension of non-network space of a catchment basin. *Geophysical Research Letters*, **31**, p. L12502.

SAGAR, B.S.D. and MURTHY, K.S.R., 2000, Generation of fractal landscape using nonlinear mathematical morphological transformations. *Fractals*, **8**, pp. 267–272.

SAGAR, B.S.D. and TIEN, T.L., 2004, Allometric power-law relationships in a Hortonian Fractal DEM. *Geophysical Research Letters*, **31**, p. L06501.

SAGAR, B.S.D., GANDHI, G. and RAO, B.S.P., 1995a, Applications of mathematical morphology on water body studies. *International Journal of Remote Sensing*, **16**, pp. 1495–1502.

SAGAR, B.S.D., VENU, M. and RAO, B.S.P., 1995b, Distributions of surface water bodies. *International Journal of Remote Sensing*, **16**, pp. 3059–3067.

SAGAR, B.S.D., OMOREGIE, C. and RAO, B.S.P., 1998a, Morphometric relations of fractal-skeletal based channel network model. *Discrete Dynamics in Nature and Society*, **2**, pp. 77–92.

SAGAR, B.S.D., VENU, M., GANDHI, G. and SRINIVAS, D., 1998b, Morphological description and interrelationship between force and structure: a scope to geomorphic evolution process modelling. *International Journal of Remote Sensing*, **19**, pp. 1341–1358.

SAGAR, B.S.D., VENU, M. and MURTHY, K.S.R., 1999, Do skeletal networks derived from water bodies follow Horton's laws? *Mathematical Geology*, **31**, pp. 143–154.

SAGAR, B.S.D., VENU, M. and SRINIVAS, D., 2000, Morphological operators to extract channel networks from Digital Elevation Models. *International Journal of Remote Sensing*, **21**, pp. 21–30.

SAGAR, B.S.D., SRINIVAS, D. and RAO, B.S.P., 2001, Fractal skeletal based channel networks in a triangular initiator basin. *Fractals*, **9**, pp. 429–437.

SAGAR, B.S.D., MURTHY, M.B.R., RAO, C.B. and RAJ, B., 2003, Morphological approach to extract ridge–valley connectivity networks from Digital Elevation Models (DEMs). *International Journal of Remote Sensing*, **24**, pp. 573–581.

SERRA, J., 1982, *Image Analysis and Mathematical Morphology* (London: Academic Press).

SNYDER, N.P., WHIPPLE, K.X., TUCKER, G.E. and MERRITTS, D.J., 2000, Landscape response to tectonic forcing: Digital elevation model analysis of stream profiles in the Mendocino triple junction region, northern California. *Geological Society of America Bulletin*, **112**, pp. 1250–1263.

STONE, R. and DUGUNDJI, J., 1965, A study of microrelief: its mapping, classification, and quantification by means of a Fourier analysis. *Engineering Geology*, **1**, pp. 89–187.

TURCOTTE, D.L., 1997, *Fractals in Geology and Geophysics* (Cambridge: Cambridge University Press).

WHIPPLE, K.X. and TUCKER, G.E., 1999, Dynamics of the stream-power river incision model: implications for height limits of mountain ranges, landscape response timescale, and research needs. *Journal of Geophysical Research*, **104**, pp. 17661–17674.

WHIPPLE, K.X., KIRBY, E. and BROCKLEHURST, S.H., 1999, Geomorphic limits to climate-induced increases in topographic relief. *Nature*, **401**, pp. 39–43.

ZEBKER, H.A. and GOLDSTEIN, R.M., 1986, Topographic mapping from interferometric Synthetic Aperture Radar observations. *Journal of Geophysical Research*, **91**, pp. 4993–4999.